UNIVERSITY OF
BATH

University of Bath

Check for updates

The effect of ozone gas sterilization on the properties and cell compatibility of electrospun polycaprolactone scaffolds

Carolina Fracalossi Rediguieri[1,2], Paul A. De Bank[3*], Maria Helena Ambrosio Zanin[4], Patrícia Leo[4], Natalia Neto Pereira Cerize[4], Adriano Marim de Oliveira[4], Terezinha de Jesus Andreoli Pinto[1]

[1] Departamento de Farmácia, Faculdade de Ciências Farmacêuticas, Universidade de São Paulo, Av. Prof. Lineu Prestes, 580–B13, Cidade Universitária, CEP 05508-000, São Paulo-SP, Brasil.

[2] Agência Nacional de Vigilância Sanitária, SIA Trecho 5, Área Especial 57, Brasília-DF, Brasil.

[3] Department of Pharmacy & Pharmacology, University of Bath, Bath, BA2 7AY, U.K.

[4] Centro de Bionanomanufatura, Instituto de Pesquisas Tecnológicas, São Paulo-SP, Brasil.

* Corresponding author: Telephone +44 (0)1225 384017; e-mail: p.debank@bath.ac.uk

Correspondence details

CR: +55 (11) 3091-3649, rediguieri@yahoo.com.br; PDB: +44 (0)1225 384017, p.debank@bath.ac.uk; MZ: +55 (11) 3767-4100, mhzanin@ipt.br; PL: +55 (11) 3767-4100, patrileo@ipt.br; NC: +55 (11) 3767-4100, ncerize@ipt.br; AdeO: +55 (11) 3767-4100, amarim@ipt.br; TP: +55 (11) 3091-3649, tjapinto@usp.br

1

The effect of ozone gas sterilization on the properties and cell compatibility of electrospun polycaprolactone scaffolds

Abstract

The growing area of tissue engineering has the potential to alleviate the shortage of tissues and organs for transplantation, and electrospun biomaterial scaffolds are extremely promising devices for translating engineered tissues into a clinical setting. However, to be utilized in this capacity, these medical devices need to be sterile. Traditional methods of sterilization are not always suitable for biomaterials, especially as many commonly used biomedical polymers are sensitive to chemical-, thermal- or radiation-induced damage. Therefore, the objective of this study was to evaluate the suitability of ozone gas for sterilizing electrospun scaffolds of polycaprolactone (PCL), a polymer widely utilized in tissue engineering and regenerative medicine applications, by evaluating if scaffolds composed of either nanofibres or microfibres were differently affected by the sterilization method. The sterility, morphology, mechanical properties, physicochemical properties, and response of cells to nanofibrous and microfibrous PCL scaffolds were assessed after ozone gas sterilization. The sterilization process successfully sterilized the scaffolds and preserved most of their initial attributes, except for mechanical properties. However, although the scaffolds became weaker after sterilization, they were still robust enough to use as tissue engineering scaffolds and this treatment increased the proliferation of L929 fibroblasts while maintaining cell viability, suggesting that ozone gas treatment may be a suitable technique for the sterilization of polymer scaffolds which are significantly damaged by other methods.

Keywords: Sterilization; PCL; Electrospinning; Ozone; Tissue Engineering; Scaffolds

1. Introduction

The development of scaffolds for tissue engineering is the objective of many researchers worldwide and the electrospinning technique is one of most promising ways of scaling up the production of such medical devices. Electrospinning of polymeric solutions produces highly porous structures composed of very thin fibres, which mimic the scale of the extracellular

matrix of biological tissues. These nanofibre scaffolds present a larger surface area and more binding sites for cell surface receptors in comparison to other types of scaffolds [1]. Therefore, in recent years, many developments have been made in the field of tissue engineering by employing electrospinning of a variety of natural and synthetic polymers. The technique allows for flexibility in the physicochemical and morphological characteristics of the scaffold, with adaptations including the generation of multilayer sheets, solid, hollow or coaxial fibres, and cylindrical or ribbon like shapes, with various diameters and pore sizes in addition to simple, single layer sheets [2, 3]. In addition, hybrid scaffolds and tissues can be generated by combining electrospinning with other fabrication techniques such as bioextrusion and 3D printing [4, 5], while blending polymers with adhesive biomolecules such as peptides or proteins can achieve enhanced cell compatibility [6-9]. Among the different polymers used in electrospun tissue engineering scaffolds, polycaprolactone (PCL) is one of the most commonly used. PCL is a biodegradable, hydrophobic polyester frequently used in 3D printers because of its low melting point [10]. It has been electrospun under many conditions, using a variety of solvents and process parameters, and has been used to construct a variety of tissues including bone, cartilage, skin, cardiovascular and nervous tissues [11-13].

According to regulatory bodies for medical products, every implantable medical device must be sterile, and the efficacy of the sterilization process must be confirmed. What is more, aseptic sterile manufacturing processes should only be employed when a terminal sterilization process is not feasible [14-16]. Traditional sterilization methods have been applied to different electrospun polymeric scaffolds. However, these processes can cause many detrimental effects by chemical- or radiation-induced damage, or when heat is either applied directly as sterilizing agent, or generated during the sterilization process. To minimize these effects, alternative methods have been emerging, including the use of ozone gas, which has an excellent sterilization capacity against a variety of microorganisms [17], and is attractive due to its low cost, use of natural inputs (oxygen), and applicability to thermosensitive materials [18].

Electrospun PCL scaffolds have been sterilized using many methods, most of them causing unwanted changes to the morphology, molecular weight or mechanical properties of the scaffolds [19]. Recently, we have demonstrated that ozone gas sterilization is a suitable method for sterilizing PLGA scaffolds without changing their physicochemical or mechanical properties [20]. In this study, we investigated if ozone gas is also applicable to PCL by comparing scaffold morphology, mechanical properties, physicochemical properties, and cell response following sterilization. Furthermore, it has been suggested that the negative effects of sterilization methods on fibres are more pronounced in thinner fibres, i.e., those with a diameter below 1 μm. Therefore, we also investigated whether ozone gas sterilization has differing effects on PCL nano- or microfibres.

2. Materials and methods

2.1 Materials

Methanol and chloroform were purchased from Fisher. Tryptone Soya Broth (TSB) was purchased from Difco Laboratories, UK, and Fluid Thioglycollate Medium (FTM) from Oxoid

Microbiology Products, U.K. L929 mouse fibroblasts were acquired from Adolfo Lutz Institute, São Paulo, Brazil. All other materials, including polycaprolactone (PCL; average molecular weight 80 kDa), were purchased from Sigma Aldrich, Brazil.

2.2 Scaffold fabrication

PCL was dissolved in chloroform/methanol (3:1) at a concentration of 8% (w/v) and in chloroform/methanol (9:1) at a concentration of 12% (w/v) by stirring overnight at 22 °C. The 8% PCL solution was transferred to a 5 mL glass syringe (Hamilton) and electrospun at 16.5 kV through a 22G stainless steel needle towards a 12 x 12 cm aluminium foil-covered collector at a distance of 15 cm from the tip of the needle. A flow rate of 1.0 mL h^{-1} was maintained using a syringe infusion pump (PHD 2000 Infuse/Withdraw, Harvard Apparatus) for a period of two hours. The 12% PCL solution was similarly electrospun at 15 kV through a 22G needle, with a flow rate of 1.5 mL h^{-1} and 13 cm collector distance, also for two hours. Three fibrous mats were independently fabricated for each PCL concentration.

2.3 Scaffold sterilization and sterility assessment

A validated ozone gas sterilization procedure for medical devices (in accordance with ISO 14937 [21]) was used to sterilize the electrospun scaffolds. A prototype sterilization chamber (supplied by Ortosintese, São Paulo, Brazil) was used to apply ozone gas through the samples in a pulsed form, as described elsewhere [20]. Scaffolds were enclosed in surgical paper and exposed to four pulses of ozone gas sterilization. Briefly, each pulse was composed of four stages: vacuum, chamber filling, plateau (20 min), and vacuum. The humidity inside the chamber was up to 95%, with positive internal pressure ranging from 0.4 to 0.8 kgf/cm2 during chamber filling and negative internal pressure ranging from -0.8 to -0.4 kgf/cm2 during vacuum. Sterilized scaffolds were aseptically cut into two pieces, placed in TSB or FTM, and incubated at 22.5 °C ± 2.5 °C and 32.5 °C ± 2.5 °C, respectively, for 14 days. Each of the triplicate scaffolds was tested.

2.4 Field emission scanning electron microscopy (FE-SEM)

The morphology of sterilized and non-sterilized electrospun PCL scaffolds was examined by FE-SEM (QUANTA 3D FEG, FEI) at an accelerating voltage of 20 kV. Prior to FE-SEM analysis, specimens were sputter-coated with gold (EMITECH SC7620) to produce a conductive surface. Three samples of each scaffold were analysed, and three images were obtained from each sample. Mean fibre diameters were determined by randomly selecting 40 fibres from the central area of each image, and measuring their diameters using ImageJ 1.47v software (National Institutes of Health, Bethesda, MD; http://rsb.info.nih.gov/ij/) [22].

2.5 Porosity

Scaffolds were cut into discs of 13 mm diameter and their thickness measured using a thickness gauge (Mitutoyo). Discs were then weighed on an analytical balance. Scaffold porosity (ε) was determined by gravimetric analysis and calculated as $\varepsilon = 100 \times (1-(\rho_{app}/\rho_{bulk}))$, where ρ_{app} was the apparent density measured by the ratio between mass and volume (ρ_{app} = mass/(thickness x area)), while ρ_{bulk} was the density of the raw materials. Duplicate measurements were performed for each of the triplicate scaffolds.

2.6 Fourier transform-infrared spectroscopy (FTIR)

Fourier transform infrared spectroscopy (FTIR) was used to assess changes in the surface chemistry of the PCL scaffolds after sterilization. FTIR spectra were obtained using an FTIR spectrometer (Nicolet 6700, Thermo Scientific) with an Attenuated Total Reflectance (ATR) accessory. For each sample, 32 scans were performed over a wavelength range of 4,000-500 cm^{-1} at a resolution of 2 cm^{-1}.

2.7 Water contact angle

PCL scaffolds were cut into squares of 1 x 1 cm and placed on glass slides. A 5 µL droplet of distilled water was carefully deposited onto each specimen and, after 60 seconds, an image of each droplet was recorded using a USB digital microscope. Water contact angles were determined using the drop_analysis plug-in for ImageJ (obtained from http://bigwww.epfl.ch/demo/dropanalysis). Three samples were analysed for each of the triplicate scaffolds.

2.8 Thermal analysis

Thermogravimetric analysis of the PCL scaffolds was conducted using a TGA/DSC 1 Star System (Mettler Toledo). Samples (approximately 4 mg) were placed in aluminium pans and heated to 500 °C at a rate of 10 °C min^{-1}, under a nitrogen gas atmosphere (100 mL min^{-1} flow rate). Thermal characteristics of the scaffolds were evaluated using differential scanning calorimetry (DSC; DSC822, Mettler Toledo). Samples (approximately 1 mg) were placed in covered aluminium pans and heated from 0 to 150 °C at a rate of 10 °C min^{-1} under a nitrogen gas atmosphere (50 mL min^{-1} flow rate), followed by cooling to 0 °C and a second heating under the same conditions and temperature range. Each of the triplicate scaffolds was analysed.

2.9 Gel permeation chromatography (GPC)

Samples of electrospun PCL scaffolds were analysed by GPC following overnight dissolution in HPLC grade chloroform and filtration through 0.45 μm membranes. Injection volumes of 200 μl were loaded on to a Waters HPLC system (comprising a W515 pump, a pump control module, degasser, W2707 autosampler, column thermostat and a W2414 refractive index detector), equipped with a set of three linked Phenomenex Phenogel™ 5μm size exclusion columns, using chloroform as the eluent at a flow rate of 1.0 mL min^{-1} and a temperature of 30 °C. Waters Empower2 software was used to determine the weight average molecular weight (Mw) and number average molecular weight (Mn) of each sample, in comparison to low-dispersity polystyrene standards.

2.10 Mechanical properties

Tensile strength and Young's Modulus of scaffolds were measured using a Universal Testing Instrument (Instron 5869). Samples were cut into 20 mm × 10 mm strips, fixed in cardboard frames and a uniaxial force applied at a rate of 8 mm min^{-1} using a 100 N load cell at 22 °C. Three samples were tested for each of the triplicate scaffolds.

2.11 Cell culture

L929 fibroblasts were cultured in Dulbecco's Modified Eagle's Medium supplemented with foetal bovine serum (10% v/v), penicillin (100 UI mL^{-1}), streptomycin (100 μg mL^{-1}) and amphotericin B (250 ng mL^{-1}) and maintained at 37 °C with 5% CO_2 in a humidified incubator.

2.12 Cell proliferation on scaffolds

To assess the biocompatibility of the sterilized PCL scaffolds, cell proliferation was measured using a resazurin assay of cell metabolic activity. Electrospun scaffolds were cut into 15 mm diameter discs, held in 48-well CellCrown inserts (Scaffdex Ltd.), placed in culture plates and incubated in culture medium for 90 minutes. Subsequently, 40 μL of a L929 fibroblasts suspension was seeded on to each scaffold at a density of 5,000 cells per disc. Cells were allowed to adhere to scaffolds for 40 minutes in this small volume before a further 900 μL of medium was carefully added to each well. Cells from the same suspension were seeded on tissue culture plastic to act as a positive control, while scaffolds in culture medium without cells were used as a negative control. Cell proliferation on the scaffolds was assessed by measuring the metabolic reduction of resazurin at various time points. An aqueous stock solution of 0.15 mg mL^{-1} resazurin sodium salt in Dulbecco's phosphate-buffered saline (pH 7.4) was prepared and filter-sterilized. At each time point, the culture medium was removed from each well and

6

replaced with 1mL fresh medium containing resazurin solution at a concentration of 10% v/v. Plates were returned to the culture incubator for 3 hours, after which 100 μL aliquots of medium were removed from each well and transferred to a 96-well microplate. The remaining medium was then removed, replaced with fresh, resazurin-free medium and the plates were returned to the incubator until the next assay time point. The fluorescence of sampled media was measured on a fluorescence plate reader (Biotek Synergy HT) with an excitation wavelength of 540 nm and emission wavelength of 590 nm. The values obtained from negative control scaffolds were subtracted to determine the fluorescent signal originating from the cellular metabolic activity. Triplicate wells were assessed for each of the triplicate scaffolds and the mean ± standard error fluorescence value at each time point determined from three independent experiments.

2.13 Cell viability on scaffolds

L929 fibroblasts were seeded on PCL scaffolds in CellCrowns as previously described and cultured for 1, 4, 7 or 12 days. At each time point, the culture medium was removed from each well and the scaffolds were washed with phosphate-buffered saline (PBS). Cells were then stained with the Live/Dead Double Staining Kit (#04511, Sigma-Aldrich), according to the manufacturer's instructions. Briefly, 350 μL of solution containing 2 μL mL^{-1} of calcein AM and 1 μL mL^{-1} of propidium iodide in PBS was added to each well and incubated for 30 minutes. Subsequently, the staining solution was removed and replaced by serum-free culture medium. Cells were observed using a fluorescent microscope (Axio Vert.A1) under excitation/emission wavelengths of 490/515 nm and 535/617 nm, for live and dead, respectively. The number of cells was counted in five fields for each scaffold, with two replicates tested for each type of scaffold.

2.14 Statistical analysis

Statistical analysis was performed using GraphPad Prism version 5.00 for Windows (GraphPad Software; www.graphpad.com). All data are reported as mean ± standard error from the independent replicates. One-way Student's t tests were used to analyse differences between groups and Mann Whitney analysis was used to compare medians. A value of $p < 0.05$ was considered statistically significant.

3. Results

3.1 Scaffold sterility

After 14 days of incubation in TSB or FTM, all tubes containing the ozone-sterilized scaffolds remained clear, indicating no microorganism growth and confirming that the electrospun PCL scaffolds were sterile after four pulses of ozone gas.

3.2 Scaffold morphology

Electrospun 8% PCL or 12% PCL scaffold mats exhibited a mean thickness of 91 ± 19 μm and 152 ± 45 μm, respectively. SEM micrographs of electrospun PCL fibres before and after ozone gas sterilization are shown in Figure 1. The electrospinning of 8% PCL resulted in fibres with diameters in the micro- to nanometre range, while 12% PCL resulted in microfibres only (Figure 1, Table 1). All fibres were bead-free and exhibited a similar morphology before and after sterilization, although there was some evidence of 8% PCL fibres merging and ribboning which was more noticeable following ozone treatment. However, there were no changes in the mean fibre diameter following sterilization (Table 1). The porosity of 8% PCL scaffolds (~89%) was higher than that of 12% PCL scaffolds (~84%; $p < 0.05$), and no change in these values was observed after sterilization (Table 1).

[Figure 1 near here]

[Table 1 near here]

3.3 Surface characterization

The water contact angle measurements of non-sterilized and sterilized scaffolds are shown in Table 1. The contact angle measurements for 8% PCL scaffolds were slightly higher than for 12% PCL, but it is evident that the sterilization process did not affect the wettability of the scaffolds as the contact angles remained unchanged. Attenuated Total Reflectance Fourier Transform Infrared Spectroscopy (ATR-FTIR) was used to explore the surface chemistry of PCL scaffolds before and after sterilization (Figure 2). The spectra show typical peaks of ester carbonyl groups (~1,720 cm^{-1}), attributable to C=O stretching, and peaks between 1,300 and 1,050 cm^{-1}, which correspond with C-O-C stretching, both present in PCL [23]. The spectra of the scaffolds before and after ozone gas treatment were very similar, with no apparent additional peaks following ozone treatment.

[Figure 2 near here]

3.4 Thermal characterization

The thermogravimetric and DSC curves of the PCL scaffolds before and after sterilization are shown in Figure 3, and the thermal properties of the scaffolds are summarized in Table 2. The thermogravimetric curves (Figure 3(a)) indicate that the thermal decomposition processes of all samples were similar and occurred in a single step, ranging from approximately 370 to 440 °C, with a weight loss of more than 91%. DSC curves of PCL scaffolds show a strong endothermic event around 59 °C, which corresponds to the melting point of the polymer (Figure 3(b)).

[Figure 3 near here]

[Table 2 near here]

3.5 Molecular mass analysis

To determine whether ozone gas sterilization affected the molecular mass distribution of PCL in the electrospun scaffolds, GPC analysis was performed and the results are shown in Table 3. Assessment of the molecular mass distributions before and after sterilization showed a significant decrease in molecular weight, molecular number and peak weight of PCL scaffolds after ozone treatment, accompanied by a significant increase in polydispersity. The greatest changes were observed in 8% PCL nanofibrous scaffolds in comparison to 12% PCL microfibrous matrices.

[Table 3 near here]

3.6 Mechanical properties

The values of tensile strength and Young's Modulus of non-sterilized and sterilized PCL scaffolds are shown in Table 4, indicating that the treatment with four pulses of ozone gas affected the mechanical properties of the scaffolds. The tensile strength of 8% PCL scaffolds reduced from 1.64 ± 0.22 MPa to 0.78 ± 0.25 MPa, while that of 12% PCL reduced from 1.87 ± 0.30 MPa to 1.06 ± 0.14 MPa. Young's Modulus appeared to increase slightly after sterilization, but the difference was not significant ($p > 0.05$).

[Table 4 near here]

3.7 Cell behaviour

To investigate the effect of ozone gas sterilization on the response of a model cell line to electrospun PCL scaffolds, the proliferation of L929 fibroblasts was examined using the resazurin reduction assay over a period of 11 days (Figure 4). Cell proliferation was greater on scaffolds treated with ozone than on non-sterilized ones, with these differences being statistically significant on days 7 and 11 for 8% PCL, and on day 11 when analysing 12% PCL. Cell viability was assessed by live/dead staining (calcein-AM and propidium iodide) at different time points up to 12 days. Figure 5 shows that the L929 fibroblasts adhered to and proliferated over both non-sterilized and sterilized 8% and 12% PCL scaffolds when observed 1, 4, 7 and 12 days after seeding. During this period, very few dead cells were observed and the viability on all scaffolds was greater than 95%, with no observable differences among the groups.

[Figure 4 near here]

[Figure 5 near here]

4. Discussion

Since ozone gas sterilization has previously been shown to be a very promising alternative method to sterilizing electrospun PLGA scaffolds [20], we decided to investigate whether it could also be effectively applied in the sterilization of other polyesters, and PCL was chosen because it is widely used in tissue engineering and other biomedical applications. Some studies in the literature have suggested that the diameter of polymer fibres can influence the potentially negative impacts of commonly used sterilization methods, with thinner fibres being more significantly adversely affected [24, 25]. Based on this evidence, we investigated whether ozone gas affected PCL nano- or microfibres differently by fabricating scaffolds from 8% PCL (obtaining fibres with a mean diameter <1 μm) and 12% PCL (obtaining with a mean diameter >2 μm) (Table 1). For both scaffold types, their sterility was tested after exposure to four pulses of ozone gas by immersing them for 14 days in either Tryptone Soya Broth, which is commonly used to cultivate fungi and aerobic bacteria, or Fluid Thioglycollate Medium, primarily intended for the culture of anaerobic bacteria [15]. These sterility tests confirmed the lack of viable bacteria or fungi in these scaffolds.

The physicochemical properties of PCL nano- and microfibres were consistent with previous studies [26, 27]. After the ozone gas sterilization process, the sterilized fibres showed some signs of fusion and beading, although fibre diameter and porosity remained unaltered (Figure 1, Table 1). This effect is likely due to changes in the polymer crystallinity, as described below, and was most noticeable on the nanofibrous 8% PCL scaffolds. This is similar to, although not as pronounced as, the results reported for peracetic acid sterilization of PCL scaffolds, which led to fused and broken fibres after treatment [28].

10

In terms of surface characteristics, ATR-FTIR spectroscopy showed that no additional functional groups were present on the scaffolds after sterilization (Figure 2). In a study by Darain *et al*, FTIR analysis of PCL films treated with UV/ozone showed a new peak at 1,600 cm^{-1}, attributed to the formation of -COOH groups [29]. In addition, a large peak at 3,400 cm^{-1} was observed on treated films, being attributable to -OH groups formed after treatment, which also increased hydrophilicity, an effect we did not observe in this study (not shown). Even though no new peaks were observed in our study, it is possible to observe a small decrease in the intensity of the peak at 1,160 cm^{-1}, which corresponds to C–O and C–C stretching of the amorphous phase [30, 31], suggesting a slight decrease in the amorphous phase of the polymer after sterilization. This effect was more noticeable in microfibres than nanofibres, and this may be due to the higher crystalline phase of microfibres when compared to nanofibres [27]. Following ATR-FTIR analysis, we then investigated the wettability of the PCL nanofibres by measuring the water contact angle. Although there was a downward trend in the water contact angle after ozone gas sterilization, this decrease was not statistically significant (Table 1). As expected from the lack of apparent surface chemistry changes visible in ATR-FTIR spectra, this demonstrates that ozone gas treatment had little effect on PCL fibre wettability.

Examination of the morphology and surface characteristics of the different scaffolds was followed by an investigation of their bulk properties using TG analysis and DSC to investigate if ozone gas sterilization altered the thermal properties of the scaffolds. The results showed that the melting temperature of nanofibrous scaffolds slightly decreased (~0.7 °C) after ozone sterilization (Table 2, second heating), which could be attributable to some chain scission after sterilization. The melting enthalpy increased in both nano- and microfibrous scaffolds after sterilization (Table 2, second heating), possibly due to an alteration of crystallinity of the scaffolds after sterilization, since the melting enthalpy is directly related to the percentage of the polymer crystallinity [32-34]. An increased percentage of crystallinity may have resulted from a decrease in the amorphous phase after sterilization, since the amorphous phase degrades faster than crystalline [35, 36]. As discussed above, the decrease in the amorphous phase could be observed in FTIR spectra, where an apparent reduction of the peak in 1,160 cm^{-1} was shown [37].

To investigate whether changes in polymer molecular mass could have affected the characteristics of the scaffolds, GPC analysis was performed on non-sterilized and ozone-sterilized scaffolds. As shown in Table 3, molecular mass significantly decreased following ozone treatment, while polydispersity significantly increased. The decrease in all measures of molecular mass, M_w, M_n and M_p, was more pronounced for 8% PCL nanofibrous scaffolds compared to 12% PCL microfibers, most likely due to the higher surface area to volume ratio of the nanofibres resulting in increased exposure to the ozone. The correlation between the increased crystallinity post-sterilization, shown in Table 2, and the decrease in molecular mass is in agreement with the literature, where it has been shown that lower molecular weight PCL is more crystalline than the higher molecular weight polymer [38]. Bosworth and Downes have also demonstrated that as PCL scaffolds degrade over time, molecular mass decreases with a concurrent increase in crystallinity, which supports our findings [39]. Interestingly, these authors also noted that the molecular mass of the PCL in their scaffolds was greater than the M_n of the supplied material (80,000 g mol^{-1}), again matching our observations [39].

Mechanical properties of scaffolds before and after sterilization were also evaluated. Four pulses of ozone gas altered the mechanical properties of both nano- and microfibrous,

decreasing the tensile strength by around 50%. Although the Young's Modulus showed no significant difference after sterilization, an increasing trend was observed. The non-uniform characteristics throughout the matrices, even though normalized by the thickness, might have contributed to the disparity of these results. Therefore, with the statistical model applied here it was not possible to conclude that there was a significant difference between the groups.

However, there is clearly an opposing effect of ozone gas treatment on the tensile strength and Young's Modulus of these electrospun PCL scaffolds. The increased crystallinity of the matrices, shown in the DSC results, is likely to be responsible for the increase in the Young's Modulus, with the higher crystallinity of the 12% PCL scaffolds correlating with a higher modulus. An increase in crystallinity would also be expected to contribute to an increase in tensile strength, but the opposite is observed in this study. However, the significant reduction in molecular mass and increase in polydispersity observed in the GPC studies following ozone treatment would be expected to reduce the tensile strength of the polymer. Therefore, the changes in both crystallinity and molecular mass are likely to contribute to the effects on scaffold mechanical properties, although a full investigation into the relative contributions of these factors is beyond the scope of this study.

In comparison with other studies on sterilization of PCL scaffolds, Bosworth *et al* found a similar trend in mechanical properties of PCL after gamma irradiation, with an increase in crystallinity and melting enthalpy [40]. A relationship between increased Young's Modulus with increasing crystallinity has been shown previously [41]. However, gamma irradiation was shown to be more detrimental to the PCL scaffolds, with a decrease in maximum stress of around 60% [40]. Another method of sterilization, ethylene oxide, has also been used in PCL scaffolds, but it turned them translucent and brittle [28]. In comparison with the electrospun PLGA scaffolds in our previous study [20], ozone sterilization has a more significant impact on the mechanical properties of PCL scaffolds. These findings are in accordance with other methods of sterilization, such as gamma radiation and ethylene oxide, that were applied to both polymers scaffolds and show the detrimental effects were more pronounced in PCL scaffolds than PLGA ones [19]. However, although the mechanical properties of the electrospun PCL scaffolds were affected by the ozone sterilization process in this study, the scaffolds remained robust; they did not become brittle and were still capable of being handled without detriment.

To determine the effect of ozone treatment on the response of cells to electrospun PCL scaffolds, we chose L929 fibroblasts as a model cell line to examine proliferation and viability. Proliferation on the scaffolds was assessed by monitoring the reduction of resazurin to resorufin by the cells over a period of 11 days to determine their relative metabolic activity on the different matrices (Figure 4). The increasing fluorescence signal over time corresponds to an increase in the number of cells. On the first and fourth days after cell seeding on PCL scaffolds, no difference was observed between non-treated and ozone-sterilized scaffolds. Nevertheless, from day 7 onwards, cells on the sterilized nanofibrous scaffolds showed markedly higher growth than on non-sterilized ones. In the case of microfibrous scaffolds, a significant difference between sterilized and non-sterilized groups could only be observed on the 11th day after initial cell seeding.

Cell viability was determined by live/dead staining at different times up to 12 days (Figure 5). At day 7 the scaffolds showed a dense cell coverage, making it difficult to visually quantify the living cells. However, as the dead cells were very few in number, it was possible to

quantify them and estimate the viability at over 95% for all scaffold types, including non-sterilized and sterilized scaffolds. Because cell viability was not affected by ozone gas sterilization, the difference observed in the metabolic activity of cells on non-sterilized and sterilized scaffolds after day 7 is not a result of cell death. The higher cell proliferation on sterilized scaffolds could be partially explained by the alteration in mechanical properties after sterilization, since it is one of the factors that influences cell growth [42]. Furthermore, a slight decrease in fibre diameter was observed after sterilization (though not statistically significant; Table 1), which could have increased inter-fibre distance and, consequently, pore sizes, allowing better flow of nutrients and gases or even cell migration [43, 44].

Besides the increase in cell proliferation, ozone sterilization could also show advantages in terms of scaffold degradation. Although not studied in this work, it is well known that PCL scaffolds degrade very slowly *in vivo* and, for some tissue engineering applications, it may be beneficial to have a faster biodegradation process [45]. The decrease in mechanical properties could be related to the decrease in molecular weight due to polymer chain scission after ozone treatment [46], a factor that accelerates polymer degradation [33, 35]. However, further studies are needed to understand the impact of ozone sterilization on the degradation rate of scaffolds.

5. Conclusion

In this study, we have demonstrated that ozone gas was able to sterilize nano- and microfibrous PCL scaffolds. Although the sterilization process somewhat affected the physicochemical and mechanical properties of the PCL scaffolds, it improved cell proliferation while maintaining cell viability, and similar effects were observed in both nano- and microfibre scaffolds after ozone gas sterilization. The changes in mechanical properties were not detrimental to the integrity of the scaffolds and this, combined with the positive effects on cell growth, it's cost-effectiveness and green nature, demonstrate that ozone sterilization has significant potential for the terminal sterilization of PCL scaffolds, as well as those of other sensitive polymers, for a wide range of tissue engineering applications or as acellular dressings for clinical use.

Acknowledgments

Disclosure statement

No potential conflicts of interest were reported by the authors.

References

1. Stevens MM, George JH. Exploring and engineering the cell surface interface. Science. 2005;310:1135–1138.

2. Barnes CP, Sell SA, Boland ED, et al. Nanofiber technology: designing the next generation of tissue engineering scaffolds. Adv Drug Deliv Rev. 2007;59:1413–1433.

3. Burger C, Hsiao BS, Chu B. Nanofibrous materials and their applications. Annu Rev Mater Res. 2006;36:333–368.

4. Gomez E, Dias J, D'Amora U, et al. Morphological and mechanical evaluation of hybrid scaffolds for bone regeneration. Adv Mater Res. 2013;749:429–432.

5. Xu T, Binder KW, Albanna MZ, et al. Hybrid printing of mechanically and biologically improved constructs for cartilage tissue engineering applications. Biofabrication. 2013;5:015001.

6. Koh H, Yong T, Chan C, Ramakrishna S. Enhancement of neurite outgrowth using nano-structured scaffolds coupled with laminin. Biomaterials. 2008;29:3574–3582.

7. Kim SE, Heo DN, Lee JB, et al. Electrospun gelatin/polyurethane blended nanofibers for wound healing. Biomed Mater. 2009;4:044106.

8. Yoo HS, Kim TG, Park TG. Surface-functionalized electrospun nanofibers for tissue engineering and drug delivery. Adv Drug Deliv Rev. 2009;61:1033–1042.

9. Dettin M, Zamuner A, Roso M, et al. Electrospun Scaffolds for Osteoblast Cells: Peptide-Induced Concentration-Dependent Improvements of Polycaprolactone. PLoS ONE. 2015;10:e0137505.

10. Chia HN, Wu BM. Recent advances in 3D printing of biomaterials. J Biol Eng. 2015;9 [cited 2017 May 9]:[14 p.]. DOI:10.1186/s13036-015-0001-4

11. Woodruff MA, Hutmacher DW. The return of a forgotten polymer-Polycaprolactone in the 21st century. Prog Polym Sci. 2010;35:1217–1256.

12. Cipitria A, Skelton A, Dargaville TR, et al. Design, fabrication and characterization of PCL electrospun scaffolds-a review. J Mater Chem. 2011;21:9419–9453.

13. Dash TK, Konkimalla VB. Poly-є-caprolactone based formulations for drug delivery and tissue engineering: A review. J Control Release. 2012;158:15–33.

14. European Commission. Council Directive 90/385/EEC on the approximation of the laws of the Member States relating to active implantable medical devices. OJ. 1990;L189:17-36.

15. World Health Organization Expert Committee on Specifications for Pharmaceutical Preparations. 45th report. Geneva, Switzerland: World Health Organization; 2011 (WHO Technical Report Series, No. 961).

16. Guidance for Industry, Sterile Drug Products Produced by Aseptic Processing - Current Good Manufacturing Practice. Washington, D.C.: U.S. Department of Health and Human Services, Food and Drug Administration; 2004.

17. Gurley B. Ozone: pharmaceutical sterilant of the future? J Parenter Sci Technol. 1985 Nov;39:256–261.

19. Moat J, Cargill J, Shone J, et al. Application of a novel decontamination process using gaseous ozone. Can J Microbiol. 2009;55:928–933.

19. Rediguieri CF, Sassonia RC, Dua K, et al. Impact of sterilization methods on electrospun scaffolds for tissue engineering. Eur Polym J. 2016;82:181–195.

20. Rediguieri CF, de Jesus Andreoli Pinto T, Bou-Chacra NA, et al. Ozone Gas as a Benign Sterilization Treatment for PLGA Nanofiber Scaffolds. Tissue Eng Part C Methods. 2016;22:338–347.

21. International Organization for Standardization (ISO). Sterilization of health care products - General requirements for characterization of a sterilizing agent and the development, validation and routine control of a sterilization process for medical devices. Geneva, Switzerland: ISO;2009. Standard No. ISO 14937:2009.

22. Schneider CA, Rasband WS, Eliceiri KW. NIH Image to ImageJ: 25 years of image analysis. Nat Methods. 2012;9:671–675.

23. Narayanan G, Aguda R, Hartman M, et al. Fabrication and Characterization of Poly(epsilon-caprolactone)/alpha-Cyclodextrin Pseudorotaxane Nanofibers. Biomacromolecules. 2016;17:271–279.

24. Duzyer S, Koral Koc S, Hockenberger A, et al. Effects of Different Sterilization Methods on Polyester Surfaces. Tekst Konfeksiyon. 2013;23:319–324.

25. Phillip EJ, Murthy NS, Bolikal D, et al. Ethylene oxide's role as a reactive agent during sterilization: Effects of polymer composition and device architecture. J Biomed Mater Res Part B Appl Biomater. 2013;101B:532–540.

26.   Lee KH, Kim HY, Khil MS, et al. Characterization of nano-structured poly(epsilon-caprolactone) nonwoven mats via electrospinning. Polymer. 2003;44:1287–1294.

27.   Rez Al MF, Elnakady YA, Fouad H, et al. Fabrication and Characterization of Polycaprolactone Micro and Nanofibers for Vascular Tissue Replacement. Sci Adv Mater. 2015;7:599–605.

28.   Yoganarasimha S, Trahan WR, Best AM, et al. Peracetic acid: a practical agent for sterilizing heat-labile polymeric tissue-engineering scaffolds. Tissue Eng Part C Methods. 201;20:714–723.

29.   Darain F, Chan WY, Chian KS. Performance of surface-modified polycaprolactone on growth factor binding, release, and proliferation of smooth muscle cells. Soft Mater. 2011;9:64–78.

30.   Elzein T, Nasser-Eddine M, Delaite C, et al. FTIR study of polycaprolactone chain organization at interfaces. J Colloid Interface Sci. 2004;273:381–387.

31.   Oliveira JE, Mattoso LHC, Orts WJ, et al. Structural and Morphological Characterization of Micro and Nanofibers Produced by Electrospinning and Solution Blow Spinning: A Comparative Study. Adv Mater Sci Eng. 2013; [cited 2017 May 9]:[14 p.]. DOI: 10.1155/2013/409572

32.   Sun M, Downes S. Physicochemical characterisation of novel ultra-thin biodegradable scaffolds for peripheral nerve repair. J Mater Sci Mater Med. 2nd ed. Springer US; 2009;20:1181–1192.

33.   Fukushima K, Feijoo JL, Yang M-C. Abiotic degradation of poly(DL-lactide), poly(ε-caprolactone) and their blends. Polym Degrad Stabil. 2012;97:2347–2355.

34.   Ribeiro Neto WA, Pereira IHL, Ayres E, et al. Influence of the microstructure and mechanical strength of nanofibers of biodegradable polymers with hydroxyapatite in stem cells growth. Electrospinning, characterization and cell viability. Polym Degrad Stabil. 2012;97:2037–2051.

35.   Tsuji H, Ikada Y. Blends of aliphatic polyesters. II. Hydrolysis of solution-cast blends from poly(L-lactide) and poly(E-caprolactone) in phosphate-buffered solution. J Appl Polym Sci. 1998;67:405–415.

36.   Eldsater C, Erlandsson B, Renstad R, et al. The biodegradation of amorphous and crystalline regions in film-blown poly(epsilon-caprolactone). Polymer. 2000;41:1297–1304.

37.   Chang H-M, Prasannan A, Tsai H-C, et al. Ex vivo evaluation of biodegradable poly(ε-caprolactone) films in digestive fluids. Appl Sur Sci. 2014;313:828–833.

38.   Jenkins MJ, Harrison KL. The effect of molecular weight on the crystallization kinetics of polycaprolactone. Polym. Adv. Technol. 2006;17:474–478.

39.   Bosworth LA, Downes S. Physicochemical characterisation of degrading polycaprolactone scaffolds. Polym Degrad Stab. 2010;95:2269–2276.

40.   Bosworth LA, Gibb A, Downes S. Gamma irradiation of electrospun poly(e-caprolactone) fibers affects material properties but not cell response. J Polym Sci Pol Phys. 2012;50:870–876.

41.   Kolbuk D, Guimond-Lischer S, Sajkiewicz P, et al. The Effect of Selected Electrospinning Parameters on Molecular Structure of Polycaprolactone Nanofibers. International J Polym Mater. 2015;64:365–377.

42.   Baker SC, Rohman G, Southgate J, et al. The relationship between the mechanical properties and cell behaviour on PLGA and PCL scaffolds for bladder tissue engineering. Biomaterials. 2009;30:1321–1328.

43.   McGlohorn JB, Holder WD, Grimes LW, et al. Evaluation of smooth muscle cell response using two types of porous polylactide scaffolds with differing pore topography. Tissue Eng. 2004;10:505–514.

44.   Hollister S. Porous scaffold design for tissue engineering. Nat Mater. 2005;4:518–524.

45.   Zhang H, Zhou L, Zhang W. Control of Scaffold Degradation in Tissue Engineering: A Review. Tissue Eng Part B Rev. 2014;20:492–502.

46.   Grosvenor MP, Staniforth JN. The effect of molecular weight on the rheological and tensile properties of poly(epsilon-caprolactone). Int J Pharm. 1996;135:103–109.

Figure 1. Representative field emission scanning electron microscopy micrographs of 8% PCL and 12% PCL electrospun scaffolds before and after ozone gas sterilization. Scale bars = 10 μm.

Figure 2. Attenuated Total Reflectance Fourier transform infrared spectroscopy spectra of non-sterilized (NS) and sterilized (ST) electrospun PCL scaffolds (four pulses of ozone gas). The dashed line highlights the peak at 1,160 cm^{-1}, which corresponds to C–O and C–C stretching of the amorphous phase.

Figure 3. Thermoanalytical characterization of non-sterilized (NS) and sterilized (ST) electrospun PCL scaffolds. Thermogravimetric curves were obtained in a nitrogen atmosphere (100 mL min^{-1}) and heating rate of 10 °C min^{-1} (a) and differential scanning calorimetry (DSC) curves were obtained in a nitrogen atmosphere (50 mL min^{-1}) and heating rate of 10 °C min^{-1} (b). Scale bars represent 50% mass loss and 2.0 W g^{-1}, respectively.

Figure 4. L929 fibroblast proliferation on non-sterilized (NS) and ozone gas-sterilized (ST) electrospun PCL scaffolds determined by the reduction of resazurin to resorufin. Data represent the mean + standard error (n = 3). * $p < 0.05$ when compared to the equivalent, non-sterilized scaffold. # $p < 0.05$ when compared to the corresponding 8% PCL scaffold.

Figure 5. Representative fluorescence microscopy images of live (green) and dead (red) cells grown on electrospun PCL scaffolds before (NS) and after (ST) ozone gas sterilization. Scale bars = 50 μm.

Table 1. Summary of morphology and surface characteristics of PCL scaffolds before and after sterilization by ozone gas. Data represent the mean ± standard error (n=3).

Scaffold	Ozone sterilized?	Mean fibre diameter (nm)	Porosity (%)	Contact angle (°)
8% PCL	No	847 ± 28	89.23 ± 0.57	131.22 ± 0.45
	Yes	769 ± 89	89.47 ± 0.52	130.59 ± 0.23
12% PCL	No	2167 ± 14 #	83.70 ± 0.51 #	127.41 ± 1.36 #
	Yes	2133 ± 156 #	84.45 ± 0.83 #	126.18 ± 1.46 #

# $p < 0.05$ when compared to the corresponding 8% PCL scaffolds

Table 2. Thermal properties of PCL scaffolds before and after sterilization with four pulses of ozone gas. Data represent the mean ± standard error (n=3).

Scaffold	Ozone sterilized?	TG Decomposition onset (ºC)	DSC First heating T_m (°C)	ΔH_m (J g^{-1})	Second heating T_m (°C)	ΔH_m (J g^{-1})
8% PCL	No	374.7 ± 0.2	58.3 ± 0.4	72.2 ± 0.6	55.5 ± 0.2	45.5 ± 0.5
	Yes	373.5 ± 0.5	58.6 ± 0.1	72.1 ± 1.7	54.8 ± 0.2 *	52.4 ± 1.0 *
12% PCL	No	375.6 ± 0.2 #	60.7 ± 0.4 #	73.5 ± 1.4	55.1 ± 0.3	48.5 ± 0.2 #
	Yes	375.0 ± 0.1 *#	60.9 ± 0.4 #	86.1 ± 2.3 *#	54.9 ± 0.4	62.3 ± 2.3 *#

T_m = melting temperature

ΔH_m = melting enthalpy

* p < 0.05 when compared to the equivalent, non-sterilized scaffold

# p < 0.05 when compared to the corresponding 8% PCL scaffold

Table 3. GPC analysis of weight average (Mw), number average (Mn) and peak (Mp) molecular weights of PCL in electrospun scaffolds before and after sterilization with ozone gas. Data represent the mean ± standard error (n=3).

Scaffold	Ozone sterilized?	Mw (g mol^{-1})	Mn (g mol^{-1})	Mp (g mol^{-1})	Polydispersity index
8% PCL	No	206,401 ± 11,143	145,812 ± 10,557	169,406 ± 15,163	1.42 ± 0.03
	Yes	119,018 ± 5,604 *	65,106 ± 3,041 *	90,000 ± 610*	1.80 ± 0.05*
12% PCL	No	177,159 ± 13,952	116,948 ± 13,364	129,544 ± 17,460	1.53 ± 0.05
	Yes	118,754 ± 2,497 *	65,430 ± 2,952 *	79,263 ± 9,332*	1.82 ± 0.05*

* p< 0.05 when compared to the equivalent, non-sterilized scaffold.

Table 4. Mechanical properties of PCL scaffolds before and after sterilization with four pulses of ozone gas. Data represent the mean ± standard error (n=3).
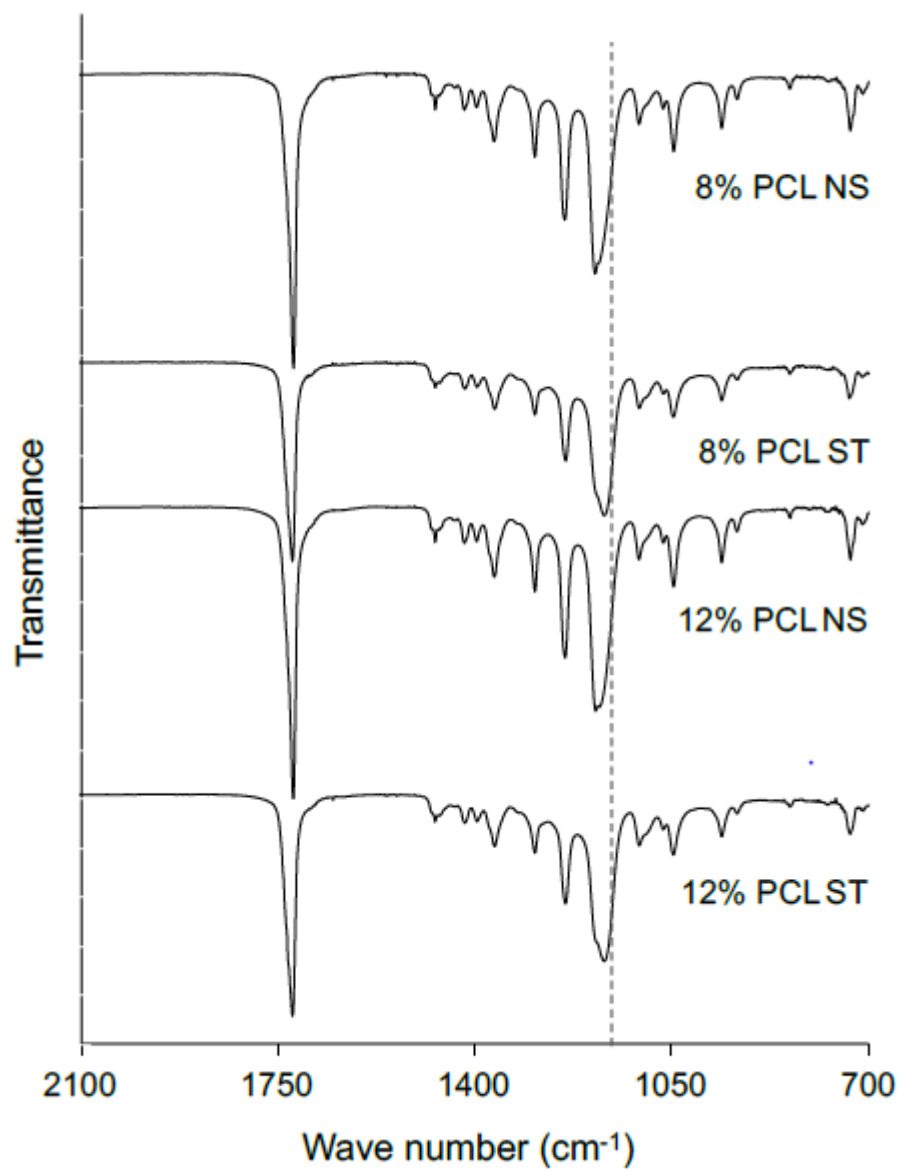
Scaffold	Ozone sterilized?	Tensile strength (MPa)	Young's Modulus (MPa)
8% PCL	No	1.64 ± 0.22	6.44 ± 0.71
	Yes	0.78 ± 0.25 *	11.27 ± 2.70
12% PCL	No	1.87 ± 0.30	8.50 ± 0.87
	Yes	1.06 ± 0.14 *	12.22 ± 1.80

* $p < 0.05$ when compared to the equivalent, non-sterilized scaffold

Non-Sterilized Sterilized

8% PCL

12% PCL